

An energy adjustable linearly polarized passively Q-switched bulk laser with a wedged diffusion-bonded Nd:YAG/Cr⁴⁺:YAG crystal

C. Y. Cho,¹ H. P. Cheng,¹ Y. C. Chang,¹ C. Y. Tang,¹ and Y. F. Chen^{1,2,*}

¹Department of Electrophysics, National Chiao Tung University, Hsinchu, Taiwan

²Department of Electronics Engineering, National Chiao Tung University, Hsinchu, Taiwan

*yfchen@cc.nctu.edu.tw

Abstract: An energy adjustable passively Q-switched laser is demonstrated with a composite Nd:YAG/Cr⁴⁺:YAG crystal by applying a wedged interface inside the crystal. The theoretical model of the monolithic laser resonator is explored to show the energy adjustable feature with different initial transmissions of the saturable absorber at the horizontal axis. By adjusting the pump beam location across the Nd:YAG crystal, the output pulse energy can be flexibly changed from 10.9 μJ to 17.6 μJ while maintaining the same output efficiency. The polarization state of the laser output is found to be along with the polarization of the C-mount pump diode. Finally, the behavior of the multi-transverse-mode oscillation is also discussed for eliminating the instability of the pulse train.

©2015 Optical Society of America

OCIS codes: (140.3480) Lasers, diode-pumped; (140.3540) Lasers, Q-switched; (140.3945) Microcavities.

References and links

1. A. Agnesi, S. Dell'Acqua, and G. C. Reali, "1.5 Watt passively Q-switched diode-pumped cw Nd:YAG laser," *Opt. Commun.* **133**(1–6), 211–215 (1997).
2. X. Y. Zhang, S. Z. Zhao, Q. P. Wang, Q. D. Zhang, L. K. Sun, and S. J. Zhang, "Optimization of Cr⁴⁺:doped saturable-absorber Q-switched lasers," *IEEE J. Quantum Electron.* **33**(12), 2286–2294 (1997).
3. Y. F. Chen and Y. P. Lan, "Comparison between c-cut and a-cut Nd:YVO₄ lasers passively Q-switched with a Cr⁴⁺:YAG saturable absorber," *Appl. Phys. B* **74**(4–5), 415–418 (2002).
4. H. X. Wang, X. Q. Yang, S. Zhao, B. T. Zhang, H. T. Huang, J. F. Yang, J. L. Xu, and J. L. He, "2ns-pulse, compact and reliable microchip lasers by Nd:YAG/Cr⁴⁺:YAG composite crystal," *Laser Phys.* **19**(8), 1824–1827 (2009).
5. Y. J. Huang, Y. P. Huang, P. Y. Chiang, H. C. Luang, K. W. Su, and Y.-F. Chen, "High-power passively Q-switched Nd:YVO₄ UV laser at 355 nm," *Appl. Phys. B* **106**(4), 893–898 (2012).
6. Y. J. Huang, C. Y. Tang, Y. S. Tzeng, K. W. Su, and Y. F. Chen, "Efficient high-energy passively Q-switched Nd:YLF/Cr⁴⁺:YAG pulsed pumping in a nearly hemispherical cavity," *Opt. Lett.* **38**(4), 519–521 (2013).
7. N. Pavel, J. Saikawa, S. Kurimura, and T. Taira, "High average power diode end-pumped composite Nd:YAG laser passively Q-switched by Cr⁴⁺:YAG saturable absorber," *Jpn. J. Appl. Phys.* **40**(3), 1253–1259 (2001).
8. J. Dong, A. Shirakawa, and K. I. Ueda, "Sub-nanosecond passively Q-switched Yb:YAG/Cr⁴⁺:YAG sandwiched microchip laser," *Appl. Phys. B* **85**(4), 513–518 (2006).
9. S. Forget, F. Druon, F. Balembois, P. Georges, N. Landru, J. P. Feve, J. Lin, and Z. Weng, "Passively Q-switched diode-pumped Cr⁴⁺:YAG/Nd³⁺:GdVO₄ monolithic microchip laser," *Opt. Commun.* **259**(2), 816–819 (2006).
10. N. Pavel, M. Tsunekane, and T. Taira, "Composite, all-ceramics, high-peak power Nd:YAG/Cr⁴⁺:YAG monolithic micro-laser with multiple-beam output for engine ignition," *Opt. Express* **19**(10), 9378–9384 (2011).
11. O. Sandu, G. Salamu, N. Pavel, Y. Dascalu, D. Chuchumishev, A. Gaydardzhiev, and I. Buchvarov, "High-peak power, passively Q-switched, composite, all-polycrystalline ceramic Nd:YAG/Cr⁴⁺:YAG lasers," *Quantum Electron.* **42**(3), 211–215 (2012).
12. J. Dong, G. Xu, J. Ma, M. Cao, Y. Cheng, K. I. Ueda, H. Yagi, and A. A. Kaminskii, "Investigation of continuous-wave and Q-switched microchip laser characteristics of Yb:YAG ceramics and crystals," *Opt. Mater.* **34**(6), 959–964 (2012).
13. M. Kaskow, J. Sulc, J. K. Jabczynski, and H. Jelinkova, "Variable energy, high peak power, passive Q-switching diode end-pumped Yb:LuAG laser," *Laser Phys. Lett.* **11**(12), 125809 (2014).
14. W. Koechner, *Solid-State Laser Engineering*, 6th edn. (Springer, 2006), Chap. 8.
15. Y. F. Chen, Y. P. Lan, and H. L. Chang, "Analytical model for design criteria of passively Q-switched lasers," *IEEE J. Quantum Electron.* **37**(3), 462–468 (2001).

16. J. J. Degnan, "Optimization of passively Q-switched lasers," *IEEE J. Quantum Electron.* **31**(11), 1890–1901 (1995).
 17. S. O. Kasap, *Optoelectronics and Photonics*, 1st edn. (Prentice-Hall, 2001), Chap. 1.
 18. A. Rapaport, S. Zhao, G. Xiao, A. Howard, and M. Bass, "Temperature dependence of the 1.06-microm stimulated emission cross section of neodymium in YAG and in GSGG," *Appl. Opt.* **41**(33), 7052–7057 (2002).
-

1. Introduction

Q-switched laser is one of the most important techniques of the solid-state laser due to its extremely high peak power pulsed output in comparison with the continuous wave (CW) laser [1–16]. Passively Q-switched (PQS) lasers, in particular, have benefits of low cost and simple design that are more attractive in applications without the requirement of accurate repetition rate [1–6]. Nowadays, the use of solid-state saturable absorber, like utilizing the Cr⁴⁺:YAG crystal, to replace the traditional dyes makes the PQS laser more reliable. Furthermore, it is vital to utilize PQS technique in the microchip laser for those applications who need compactness, short pulse width and the lack of complex electronic control system [7–12]. However, the PQS laser has nearly constant output pulse energy in a given configuration of the laser resonator. The lack of flexible adjusting of the output pulse energy, peak power as well as the pulse duration will limit its possible applications compared to high repetition rate actively Q-switched lasers.

Recently, Kaskow et al. has demonstrated a variable energy PQS laser by changing the pump area parameter [13]. More specifically, the effective pump area can be adjusting by controlling the defocusing of the pump beam waist on the gain medium with a given laser resonator. With the tuning of the defocusing, the PQS laser output pulse energy can be changed from 0.145 mJ to 0.51 mJ. However, although the absorption efficiency of this laser was measured to be nearly equal, the defocusing of the pump spot normally comes with the disadvantage of conversion efficiency degradation. Furthermore, changing the pump spot size may not result in a variation of the cavity mode area in a classical laser cavity. As a result, it is of great interest to investigate another method to adjust the PQS output pulse energy with a given resonator.

In this work, we provide a new method to generate an energy adjustable PQS laser with equal conversion efficiency in a same configuration. A composite Nd:YAG/Cr⁴⁺:YAG crystal with a wedged bonded interface is utilized for adjusting the initial transmission of the saturable absorber. By simply changing the transverse location of the pump laser diode, the output pulse energy, peak power and pulse width can be flexibly adjusted. For the compactness design, the laser resonator is coated on two facets of the composite crystal and a C-mount laser diode is directly bottom pumping the laser crystal. We first theoretically analysis the feasibility of the energy adjustable feature for the PQS laser with rate equations. The internal transmission on the interface is also discussed to prove that it has no internal loss with such wedged diffusion-bonded interface. The initial transmission of the Cr⁴⁺:YAG crystal varied from 89.2% to 80.9% for the pump-beam locations used in the experiment. At this region, we obtain variable output pulse energy, peak power and pulse width in ranges from 10.9 μ J to 17.6 μ J, from 1.45 kW to 5.40 kW and from 4.4 ns to 2.3 ns. With the incident pump power of 1.5 W, the average output power of the PQS laser maintain at approximately 150 mW with the variation of the output pulse energy. The theoretical analysis has good agreement with the experimental result. We found that the PQS output polarization was along with the polarization of the C-mount pump diode. Finally, we investigate the temporal behavior of the laser for eliminating the instability of the output pulse. It is found that with the incident pump power higher than 1.9 W, the output pulse appears with a satellite pulse and the peak-to-peak stability become worse. We believe that the instability comes from the multi-transverse-mode output due to the thermal effect from the pump source. The output transverse distribution is further found to display an elliptical shape along the fast axis of the laser diode, which support the idea of multi-transverse-mode output.

2. Experimental setup

Figure 1(a) schematically depicts the experimental setup for the bulk PQS laser. For the laser output, we directly utilized a diffusion-bonded Nd:YAG/Cr⁴⁺:YAG crystal coated with monolithic laser cavity. The doping concentration of the Nd:YAG crystal was 1.1 at. %. The length of the composite crystal was approximately 5.5 mm and the transverse aperture was 3 × 3 mm². The first facet of the crystal was coated to be high-reflective (HR, R > 99.9%) at 1064 nm and high-transmittance (HT, T > 95%) at 808 nm. The second facet of the crystal was coated with partial reflective (PR, R = 85%) at 1064 nm. To adjust the output pulse energy of the PQS laser, the bonded interface of the composite medium was designed with a 61.2 degree. As a result, the length of the saturable absorber, l_s , would be different along the horizontal axis, x , and the initial transmission can be flexibly varied by changing the pump-beam position along x . We can express the initial transmission of the Cr⁴⁺:YAG crystal, T_0 , depended on x as [14]

$$T_0(x) = \exp[-n_g \sigma_{gs} l_s(x)], \quad (1)$$

where n_g was the ground state density of the saturable absorber and σ_{gs} was the ground state absorption cross section of the saturable absorber. $l_s(x)$ was the length of the saturable absorber depended on x , which can be shown as

$$l_s(x) = l_{s0} + x \cot(\theta), \quad (2)$$

where l_{s0} was the length of the saturable absorber at the short edge and θ was the wedged angle of the composite crystal on the bonded interface. In our experiment, l_{s0} was designed to be approximately 1 mm. Hence, from Eq. (1), the length of the Cr⁴⁺:YAG crystal, $l_s(x)$, was in a range from 1 mm to 2.648 mm corresponding to $x = 0$ mm to 3 mm. Since the initial transmission of the saturable absorber at the center, $x = 1.5$ mm, was designed to be approximately 85%, n_{gs} can be determined as $1.024 \times 10^{18} \text{ cm}^{-3}$ with $\sigma_{gs} = 8.7 \times 10^{-19} \text{ cm}^2$ [15]. As a result, the initial transmission depended on x can be found to change from 91.5% to 78.9%. Figure 1(b) demonstrates the photo of the composite crystal and the theoretical result of the initial transmission is shown in Fig. 2. For the pump source, we used a 100- μm C-mount 808-nm 3-W laser diode for the compactness design. The composite crystal and the laser diode were both mounted on the copper holder with indium foil to enhance the heat dissipation. The laser crystal was directly bottom pumped by the laser diode with a distance less than 0.5 mm.

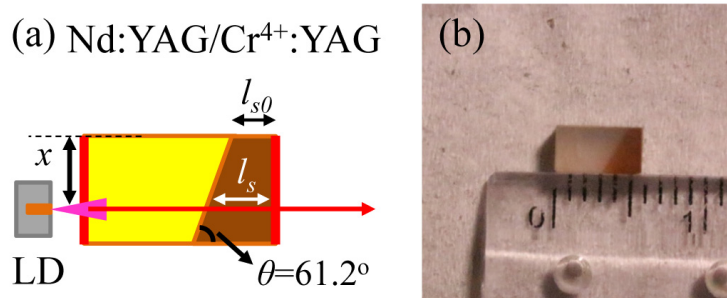


Fig. 1. (a) The experimental setup for the energy adjustable bulk PQS laser. (b) The photo of the composite crystal.

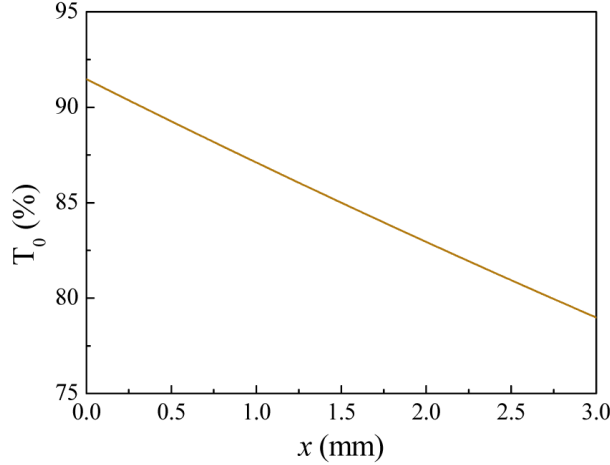


Fig. 2. The calculated result for the initial transmission of the wedged saturable absorber with respect to the pump location, x .

To investigate the feasibility of the energy adjustable feature of the PQS micro-laser, we utilized the PQS rate equation for theoretically analyzing the output performance depended on x . The output pulse energy of the PQS laser can be given by [15]

$$E_{out}(x) = \frac{h\nu A}{2\sigma} \ln \frac{1}{R} \frac{(1-\beta) \ln \frac{1}{T_0(x)^2}}{\beta \ln \frac{1}{T_0(x)^2} + \ln \frac{1}{R} + L} \left[1 - \left(\frac{T_0(x)}{(T_0)_{upper}} \right)^\eta \right] f(\alpha, \beta), \quad (3)$$

where h was the Plank constant, ν was the emission frequency, A was the emission area on the laser gain medium, σ was the absorption cross section of the Nd:YAG crystal, R was the output reflectivity, and L was the roundtrip internal loss. The parameter α and β can be given by

$$\alpha = \frac{A \sigma_{gs}}{A_s \sigma}, \quad (4)$$

$$\beta = \sigma_{es} / \sigma_{gs}, \quad (5)$$

where A_s was the emission area on the saturable absorber, σ_{es} was the excited state absorption cross section of the saturable absorber. $(T_0)_{upper}$ was the upper bound of the saturable absorber for producing a giant pulse with a given $\ln(1/R) + L$, a given α and a given value of β , which can be shown as

$$(T_0)_{upper} = \exp \left[-\frac{\ln \frac{1}{R} + L}{2(\alpha(1-\beta) - 1)} \right]. \quad (6)$$

Parameters η and $f(\alpha, \beta)$ were analytical fitting functions for the PQS laser that can be found in Ref. 15. On the other hand, the output peak power can be evaluated as [15,16]

$$P_{peak} = \frac{h\nu A}{2\sigma} \ln \frac{1}{R} \frac{c}{2nl_{cav}} \left\{ (1-\beta) \ln \frac{1}{T_0(x)^2} \left[1 - \frac{1}{\alpha} \left[1 - \left(\frac{n_t}{n_i} \right)^\alpha \right] \right] + \left(\beta \ln \frac{1}{T_0(x)^2} + \ln \frac{1}{R} + L \right) \ln \frac{n_t}{n_i} \right\}. \quad (7)$$

where n was the reflective index of the YAG crystal, l_{cav} was the cavity length that equal to the length of the composite crystal and c was the speed of the light. n_r/n_i can be calculated from the rate equation as a function of β , $T_0(x)$ and $\ln(1/R) + L$, i.e.,

$$n_r/n_i = \left(\beta \ln \frac{1}{T_0(x)^2} + \ln \frac{1}{R} + L \right) / \left(\ln \frac{1}{T_0(x)^2} + \ln \frac{1}{R} + L \right). \quad (8)$$

The theoretical results will be discussed in the next section with the experimental results.

Finally, we can further analyze the transmission through the interface of the composite crystal because the index between Nd:YAG and Cr⁴⁺:YAG crystals would exist a slightly difference. The reflectance of the TE wave and TM wave on the surface can be given by [17]

$$r_{TE} = \frac{\cos(\theta_i) - \sqrt{n_i^2 - \sin^2(\theta_i)}}{\cos(\theta_i) + \sqrt{n_i^2 - \sin^2(\theta_i)}}, \quad (9)$$

$$r_{TM} = \frac{\sqrt{n_i^2 - \sin^2(\theta_i)} - n_i^2 \cos(\theta_i)}{\sqrt{n_i^2 - \sin^2(\theta_i)} + n_i^2 \cos(\theta_i)}, \quad (10)$$

where θ_i was the incident angle, which was equal to $\pi/2 - \theta$ in our experiment, and $n_i = n_2/n_1$ was the index ratio of two materials. With Eq. (9) and (10), the transmission through the interface for two polarizations can then be evaluated as $T_{TE} = 1 - |r_{TE}|^2$ and $T_{TM} = 1 - |r_{TM}|^2$. Using n_i equal to 1.82 [18], it can be calculated that even the index difference between the Nd:YAG and the Cr⁴⁺:YAG crystals was up to 0.05, the transmission through the interface was still higher than 99.9% for both waves. This result showed that the wedged interface inside the composite crystal had nearly no internal loss for the laser oscillation. In the next part, we demonstrated the PQS laser and compared experimental results with the theoretical model.

3. Experimental results

At first, we operated the pump source above the threshold, approximately 1.8 W, to observe the energy adjustable feature of the PQS laser. We discovered that the polarization state of the PQS laser was linearly polarized, which depend on the polarization of the C-mount pump diode. The polarization ratio was measured to be approximately 90. It was worth to mention that the absorption ratio would change with the variation of the pump position since the length of the Nd:YAG crystal was different. On the other hand, the overlap between the pump beam and the laser beam became worse when the pump light propagate along the gain medium due to the large output divergence of the C-mount diode. As a result, the absorption varied with the pump position was neglected because of the inefficient pumping at the bonded area of the composite crystal. The average output power was found to be approximately 150 mW for the pump location changed from $x = 0.5$ mm to 2.5 mm. We experimentally observed that when the pump location was beyond this region, the average output power of the PQS laser drop immediately. As a result, the following experiment were operated in the region of $x = 0.5$ mm to 2.5 mm. At this region, the pump threshold was found to vary from approximately 1.51 W to 1.12 W. We experimentally observed that the output power was nearly unchanged with different pump positions when the pump power was high than 1.7 W. From Fig. 2 and with Eq. (1), we can obtain that the initial transmission of the saturable absorber was in a range from 89.2% to 80.9%. The output pulse energy of the PQS laser was calculated by the ratio of the average output power and the repetition rate observed in the experiment. We recorded the temporal behaviors of the PQS laser with a LeCroy digital oscilloscope (Wavepro 7100, 10 G samples/s, 1 GHz bandwidth) and a fast InGaAs photodiode. On the other hand, the output peak power can be calculated from the ratio of the pulse energy and the integrated area of the

pulse shape recorded by the digital oscilloscope. The comparison between the experimental results and the theoretical analysis of output pulse energy and the output peak power with respect to x are demonstrated by red points and blue curves in Fig. 3. When we adjusted the pump location from $x = 0.5$ mm to 2.5 mm, the output pulse energy was found to change from 10.9 μJ to 17.6 μJ corresponding to the repetition rate from 13.7 kHz to 8.5 kHz and the output peak power was changed from 1.45 kW to 5.40 kW. It shows great agreement between the experimental results and the theoretical analysis. The parameters used in the theoretical analysis were $\sigma_{gs} = 8.7 \times 10^{-19} \text{ cm}^2$ [15], $\sigma_{es} = 2.2 \times 10^{-19} \text{ cm}^2$ [15], $\sigma = 2.35 \times 10^{-19} \text{ cm}^2$ [18], $R = 0.85$, $l_{cav} = 5.5 \text{ mm}$, $A = A_s = 2.4 \times 10^{-4} \text{ cm}^2$, $L = 0.003$, and $n = 1.82$ [18]. The emission area on the Nd:YAG crystal and the Cr⁴⁺:YAG crystal were assumed to be the same with the pump area since the cavity was a plane-parallel resonator and the resonator was relatively short. We calculated the pump area by the divergence angle of the C-mount laser diode, approximately 35 degree and 10 degree on the fast and the slow axes, respectively, and the distance between the diode and the composite crystal. The value of the roundtrip internal loss was a fitting parameter. The output pulse width measured from the pulse shape is plotted in Fig. 4. We experimentally observed that with the increasing of the output pulse energy, the output pulse width was decreased from 4.4 ns to 2.3 ns. The temporal pulse shape with $x = 2.5$ mm is shown in the inset of Fig. 4.

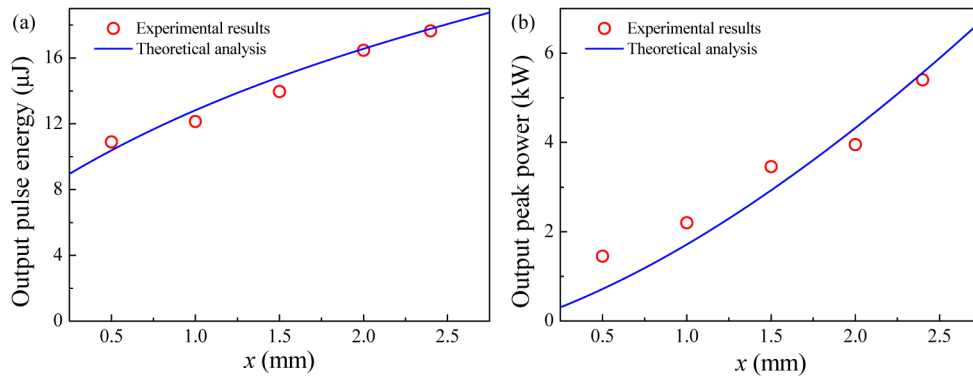


Fig. 3. The experimental result and the theoretical analysis of (a) the output pulse energy and (b) the output peak power with respect to the pump location, x .

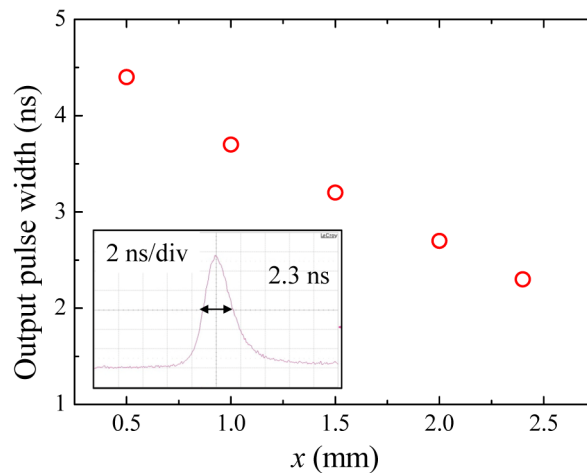


Fig. 4. The experimental result of the output pulse width with respect to the pump location, x . The inset: the temporal pulse shape of the PQS laser with pump location $x = 2.5$ mm.

Finally, the temporal behavior of the PQS laser was also investigated. Figures 5(a) and 5(b) describes the pulse train and the pulse shape of the PQS laser operated at the incident pump power of 1.9 W with $x = 2.5$ mm. The repetition rate was up to 11.6 kHz with the average output power of 200 mW and the pulse train was quite stable. However, when the pump power was higher than 1.9 W, the peak-to-peak stability of the pulse train became unstable. Furthermore, a satellite pulse appeared after the main pulse. The pulse train and the pulse shape with incident pump power of 2.2 W are depicted in Figs. 5(c) and 5(d). We also discovered that the average output power with different pump position was varied from 360 mW to 290 mW corresponding to x from 0.5 mm to 2.5 mm at the incident pump power of 2.2 W. We believed that the unstable pulse train and the satellite pulse come from the oscillation of high order transverse mode caused by the thermal effect with higher pump power. It was also believed that the output-power difference was induced by the instability of the temporal pulse behavior with different x because of variant thresholds of high order transverse modes. Figure 6 shows the average output power with respect to the incident pump power at $x = 2.5$ mm. The threshold of the PQS laser was found to be approximately 1.3 W and the slope efficiency was 32%. From insets in Fig. 6, we can further find that the transverse pattern was slightly elliptical when the input power was higher than 1.9 W. Since the elliptical shape of the pattern was along the fast axis of the laser diode, it can prove that the laser was suffering from multi-transverse-mode output.

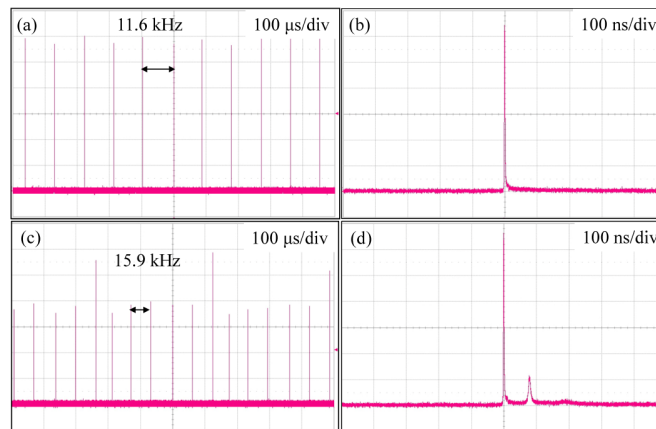


Fig. 5. The pulse train and the pulse shape of the PQS laser with pump location $x = 2.5$ mm when the incident pump power (a), (b) lower than 1.9 W and (c), (d) higher than 1.9 W.

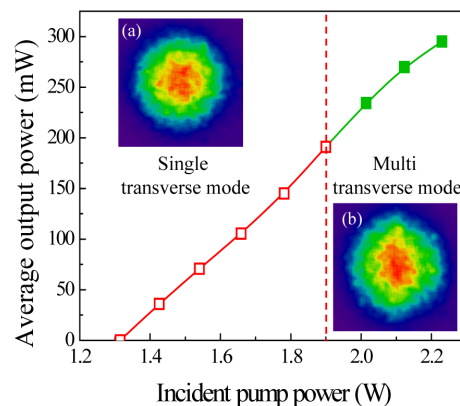


Fig. 6. The average output power with respect to the incident pump power at pump location $x = 2.5$ mm. The inset: the transverse mode distribution for the incident pump power (a) lower than 1.9 W and (b) higher than 1.9 W.

4. Conclusion

In conclusions, we demonstrate an energy adjustable bulk PQS laser with a composite Nd:YAG/Cr⁴⁺:YAG crystal. The design idea is utilizing a wedged interface inside the diffusion-bonded crystal for changing the initial transmission of the saturable absorber. We first theoretically analyze the feasibility of the energy adjustable ability for the bulk laser with rate equations. By adjusting the pump spot position from $x = 0.5$ mm to 2.5 mm, the output pulse energy and the output peak power of the PQS laser can be changed from 10.9 μ J to 17.6 μ J and from 1.45 kW to 5.40 kW corresponding to the initial transmission of the Cr⁴⁺:YAG from 89.2% to 80.9%. The theoretical model is found to have great agreement with the experimental results. We experimentally observe that the output pulse width is changed from 4.4 ns to 2.3 ns with $x = 0.5$ mm to 2.5 mm. Furthermore, the laser output is found to be linearly polarized and depends on the pump diode. The linearly polarized feature is attractive for the application of the nonlinear transformation. Finally, the temporal performance depends on the incident pump power is further discovered. We find that at a higher pump power, larger than 1.9 W, a satellite pulse will appear and the peak-to-peak stability will tend to be unstable. The reason is believed to be the oscillation of the high order transverse mode induced by serious pump intensity since the mode pattern is found to be more elliptical along the fast axis of the laser diode at higher pump power. The slope efficiency of the bulk laser is found to be approximately 32%.

Acknowledgments

The authors thank the National Science Council for the financial support of this research under Contract No. MOST 103-2112-M-009-0016-MY3.